Soft Matter

Polyelectrolyte-Micelle Coacervates: Intrapolymer-Dominant vs Interpolymer-Dominant Association, Solute Uptake and Rheological Properties

Journal:	*Soft Matter*
Manuscript ID	SM-ART-10-2018-002229.R2
Article Type:	Paper
Date Submitted by the Author:	23-Feb-2019
Complete List of Authors:	Zhao, Mengmeng; University of Akron, Polymer Engineering Wang, Chao; University of Akron, Polymer Engineering Jiang, Haowei; University of Akron, Polymer Engineering Dawadi, Mahesh; The University of Akron, Chemistry Vogt, Bryan; University of Akron, Polymer Engineering Modarelli, David; The University of Akron, Department of Chemistry Zacharia, Nicole; University of Akron, Polymer Engineering

Journal Name

ARTICLE

Polyelectrolyte-Micelle Coacervates: Intrapolymer-Dominant vs Interpolymer-Dominant Association, Solute Uptake and Rheological Properties

Received 00th January 20xx,
Accepted 00th January 20xx

DOI: 10.1039/x0xx00000x

www.rsc.org/

Mengmeng Zhao,[a] Chao Wang, [a] Haowei Jiang, [a] Mahesh B. Dawadi, [b] Bryan D. Vogt, [a] David A. Modarelli[b] and Nicole. S. Zacharia*,[a]

The effects of polyelectrolyte charge density, polyelectrolyte-to-surfactant ratio, and micelle species on coacervation were studied by turbidity, dynamic light scattering, and zeta potential measurements to examine the coacervation of the weak polyelectrolyte branched polyethylenimine (BPEI) and oppositely charged sodium dodecyl sulfate (SDS) micelles as well as BPEI and mixed micelles composed of SDS and poly(ethylene glycol) 4-nonylphenyl 3-sulfopropyl ether potassium salt (PENS). The results of dynamic light scattering and zeta potential measurements are discussed in terms of pH and BPEI-to-surfactant ratio. An intrapolymer-dominant to interpolymer-dominant association model for the BPEI-micelle coacervates was proposed based on the variation of size and zeta potential of coacervate particles by their BPEI-to-surfactant ratio. The partition coefficient of solutes into BPEI-micelle coacervates was determined using UV-vis measurement as a function of pH, BPEI-to-surfactant ratio, and mixed micelle composition. Both the hydrophobicity of solutes and micelles, as well as the association mode of coacervates, impact the solute uptake efficiency. Dynamic rheological measurements on the coacervates suggest that the rheological properties of the complex coacervates are impacted by the association mode of the coacervates as well as the charge density on BPEI chains during coacervation.

1. Introduction

The association of polyelectrolytes with oppositely charged micelles has been long known to give rise to the formation of soluble complexes or to lead to a phase separation, either liquid-liquid phase separation (complex coacervation) or liquid-solid phase separation (precipitation).[1–4] Coacervation is a phenomenon in which a macromolecular aqueous solution separates into two immiscible liquid phases.[2,5] The polymer rich dense phase, which is concentrated in macromolecules, is called the coacervate, while the other is a relatively dilute, water rich, phase. Polyelectrolyte-micelle coacervation can be easily influenced by a variety of factors including micelle properties, such as size and surface charge density; polymer properties, such as molecular weight, linear charge density and molecular geometry; polymer to micelle stoichiometry; ionic strength; and temperature.[6–8] Polyelectrolyte-micelle complexes are of great interest and importance because of their unique properties that enable potential applications, such as hydrophobic core of micelles capable of drug loading and delivery[9] and smart response to CO_2/N_2 [10], light[11,12] or temperature[13,14] stimuli. Although all polyelectrolyte-surfactant mixtures are at times referred to as complexes without regard to whether a phase separation occurred,[15,16] here materials formed when the mixing of surfactant and polyelectrolyte leads to a phase separation are referred to as coacervates.

Complex coacervation provides a route to the compartmentalization of chemical reactants, nanoparticles, as well as proteins within the microscale water-filled environments.[17–20] This compartmentalization or partitioning can be of interest for multiple reasons; to load pharmaceutical compounds into pH-sensitive coacervates for drug delivery purposes,[20] to concentrate and remove dilute contaminants from aqueous solutions,[17,19,21] to selectively purify proteins,[22] as well as to serve as a non-membrane bound protocell for origin of life studies.[23]

Membrane-bounded microcompartments in the form of self-assembled bilayer vesicles,[24–26] polymer capsules,[21,27] and inorganic vesicles[28,29] have been widely examined to compartmentalize solutes, and therefore might be appropriate as a microreactor or proposed as a protocell model. However, some key processes such as chemical or enzymatic reaction within the membrane-bounded microcompartments can be limited by the poor permeability of the membrane.[30,31] This transport limitation may inhibit the continuous chemical activity within the microcompartments due to the limitation of mass transfer of reagents to those microcompartments. In this regard, spontaneous complex coacervation provides a simple and versatile alternative procedure for compartmentalization, but without a membrane, theoretically resulting in higher permeability. In addition to that, the low surface tension between the macromolecule-rich and water-rich phases can facilitate the transfer of small molecules into the coacervate phase.[32]

[a] Department of Polymer Engineering, University of Akron, 250 S. Forge St, Akron, OH 44325, USA. E-mail: nzacharia@uakron.edu
[b] Department of Chemistry, University of Akron, Akron, Ohio 44325, United States
†Electronic Supplementary Information (ESI) available. See
DOI: 10.1039/x0xx00000x

Specific intermolecular interactions, such as electrostatics, hydrogen bonding, π-π stacking, as well as hydrophobic interactions, between the solutes and macromolecules in the coacervate droplets strongly influence the ability to partition solutes into specific complex coacervate phases. For example, our previous study on the sequestration of a cationic dye, methylene blue (MB), into complex coacervates composed of oppositely charged polyelectrolytes showed that this process is highly dependent on electrostatic and π-π interactions. Specifically, complex coacervate materials capable of forming both electrostatic and π-π interactions with the solute show a significantly higher sequestration for aromatic dye molecules than those capable of electrostatic interactions only.[17,33] In addition, another study on a hydrogen-bonding coacervate system indicates that the formation of hydrogen bonding between solutes and polymer or increase in hydrophobicity within the coacervate droplets facilitate the uptake of solutes into coacervates.[17] Micelles are well-known for their nonpolar core which allows an enhancement of solubility of hydrophobic materials.[34–36]

Complexation of polyelectrolyte with surfactant has been extensively explored with the focus on the factors that impact the size and phase behaviour of the polyelectrolyte-surfactant complexes, including polyelectrolyte molecular weight,[7,37] polyelectrolyte charge density,[38] concentration,[39] micelle surface charge density,[40–42] surfactant chain length,[37] polyelectrolyte-to-surfactant ratio,[43] ionic strength[44] and temperature.[45] Additionally, the literature does contain examples of work regarding the complexation of polyethylenimine (PEI) with SDS. As an example, Mezei *et al*. observed that different mixing protocols of PEI with SDS can have a significant impact on the size distribution and phase behavior of the PEI-SDS complexes.[15] Another study on the interaction of PEI with SDS at a concentration of SDS lower than its critical micelle concentration (CMC) reveals that an increase in the hydrophobicity and a decrease in the zeta potential of the complex particles can lead to the precipitation of the complexes.[46] The impact of NaCl concentration on the phase behavior of PBEI and SDS has also been investigated, showing that a moderate salt concentration reduces the composition range over which BPEI-SDS complexes are kinetically stable.[47]

Recently, the removal of dyes from solutions has gained increasing attention as the industry are required to lower the colour content in their wastewater. A study on the removal of dyes from solutions by polyelectrolyte-surfactant complexes indicates that the charge of the system is the most important property that influences flocculation behavior and therefore the dye sequestration.[48] Another study using chitosan hydrogel beads impregnated with carbon nanotubes shows that the incorporation of carbon nanotubes significantly enhances the removal of congo red in solution.[49]

Although a large number of studies have examined the complexation of polyelectrolyte-surfactant system and specifically the complexation of PEI and SDS, much less attention has been paid to the systematic study of the impact of BPEI charge density, BPEI to SDS ratio and the introduction of anionic mixed micelles on the size and phase behavior of BPEI-SDS complexes. In addition, though there are a variety of studies on the removal of dyes from wastewater, most of the studies lack the comparison of the sequestration efficiency of different dyes into complexes prepared at various conditions, and an in-depth study on the driving forces for the sequestration of these dyes.

Presented here is a study of how the polymer charge density (controlled by solution pH), polymer to surfactant ratio, and composition of mixed micelles can influence complex coacervation, as well as dye uptake and rheological properties of polyelectrolyte-micelle and polyelectrolyte-mixed micelle coacervates. The complex coacervate materials were formed simply by mixing a weak polyelectrolyte, branched polyethylenimine (BPEI) and oppositely charged sodium dodecyl sulfate (SDS) micelles or mixed micelles composed of sodium dodecyl sulfate (SDS) and poly(ethylene glycol) 4-nonylphenyl 3-sulfopropyl ether potassium salt (PENS). With the introduction of PENS into a BPEI-SDS coacervate system via formation of mixed SDS/PENS micelles, the hydrophobicity within the complex coacervate and therefore the hydrophobic solute encapsulation efficiency is supposed to be enhanced, as both the phenyl group and longer tails of PENS contribute to the micelle hydrophobicity.[35,36,50,51] The introduction of PENS can also allow for different types of interactions between a dye (or other molecule to be encapsulated) and the coacervate material than just electrostatic (e.g. π-π stacking). The influence of pH or charge density of BPEI on the phase behaviour of BPEI-surfactant system was qualitatively determined by turbidity measurements. The role of pH and BPEI to surfactant ratio on the complexation of BPEI and micelles was determined by dynamic light scattering (DLS) and zeta potential measurements. To better explain the variation of coacervate size and zeta potential with BPEI/surfactant mixing ratio, an intrapolymer-dominant vs interpolymer-dominant association model was proposed. The partition coefficient of dyes into the formed coacervates was determined from UV-vis spectroscopy, which shows that the partition coefficient is dependent on both the hydrophobicity of solutes and the number of micelles per BPEI chain in the coacervate. By using mixed SDS/PENS micelles instead of SDS micelles, the partition coefficient of MB into coacervates can be enhanced due to the more hydrophobic

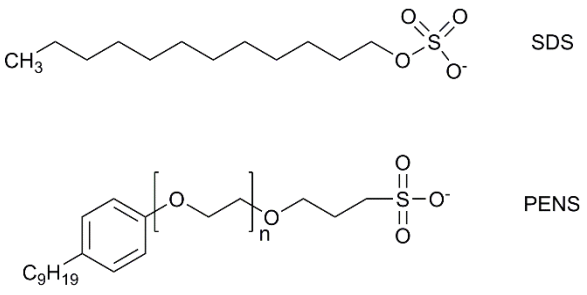

Fig. 1 Chemical structures of SDS and PENS.

environment produced by PENS. In addition to that, dynamic measurements of the coacervates show that the rheological properties of the complex coacervates are impacted by the

association mode of the coacervates as well as the charge density of the BPEI chains.

2. Experimental methods

2.1 Materials

Sodium dodecyl sulfate (SDS), Poly(ethylene glycol) 4-nonylphenyl 3-sulfopropyl ether potassium salt (PENS) and branched polyethylenimine (BPEI, $M_n = 10000$ g/mol, $M_w = 25000$ g/mol) were purchased from Sigma-Aldrich. The chemical structures of SDS and PENS are shown in Fig. 1. Dyes including methylene blue (MB), Janus green B (JGB), fluorescein sodium salt (FL) and Sudan II were purchased from Sigma-Aldrich. 9-Methylanthracene (9-MeA) and Tris(2,2'-bipyridyl)dichlororuthenium(II) hexahydrate ($Ru(bipy)_3^{2+}$) were purchased from Sigma-Aldrich. Copper (II) chloride dehydrate ($CuCl_2.2H_2O$) was purchased from Alfa Aesar. All water was dispensed from a Milli-Q water system at a resistivity of 18.2 MΩ.cm. All these materials were used as received without further purification.

2.2 Preparation of Coacervates

Stock solutions of BPEI (40 × 10^{-3} M) and SDS (40 × 10^{-3} M) with pH adjusted to 3.0, 6.0 and 9.0 were prepared separately. BPEI-SDS coacervates were formed simply by mixing the BPEI and SDS stock solutions with the same pH at different mixing ratio, keeping the total concentration of BPEI and SDS fixed at 40 × 10^{-3} M. For the formation of coacervates using BPEI and mixed micelle of SDS and PENS (BPEI-(SDS/PENS)), stock solutions of BPEI (40 × 10^{-3} M) and mixtures of SDS and PENS (SDS/PENS) with varying SDS to PENS ratio (total concentration at 40 × 10^{-3} M) were prepared at pH of 6.0. BPEI-(SDS/PENS) coacervates or soluble complexes were prepared by mixing the BPEI and SDS/PENS stock solutions at pH 6.0, with a mixing molar ratio of BPEI : (SDS/PENS) = 0.5.

2.2 Turbidity measurement

Turbidity was used to qualitatively measure the extent of coacervate formation as a function of BPEI-to-SDS stoichiometry (BPEI/SDS), charge ratio of BPEI to SDS (+/-) and pH. Turbidity measurements were performed using a 2 cm path length fiber-optic colorimeter (Brinkmann PC 950) at a wavelength of 420 nm. Turbidity was reported as 100 – *T*%, where *T* corresponds to the transmittance. Stock solutions of BPEI (40 × 10^{-3} M) and SDS (40 × 10^{-3} M) at pH 3.0, 6.0 and 9.0 were prepared separately. Titration of BPEI stock solution into SDS stock solution was done with stirring. The transmittance (T) was recorded at 60 s after each titration of BPEI.

2.3 Zeta potential measurement

Zeta potential measurement of the as-prepared BPEI-SDS and BPEI-(SDS/PENS) coacervates following method described in Section 2.2 was performed using Zeta PALS instrument (Brookhaven, USA). Each measurement was repeated for at least 3 times. The electrophoretic mobility of the complex coacervate was converted into zeta potential using Smoluchowski equation.

2.4 Dynamic light scattering

Dynamic light scattering measurements of the coacervates prepared using the method illustrated in section 2.2 were performed using a Zeta PALS instrument (Brookhaven, USA). Each measurement was repeated for at least 3 times.

2.5 Determination of partition coefficient of dyes into coacervates

After the preparation of coacervates following method in Section 2.2, 0.3 mL of 1 × 10^{-3} M MB, JGB or FL with the same pH as the polyelectrolyte solution was added to 29.7 mL BPEI-SDS coacervate system. For the mixed micelle containing coacervates, 0.3 mL 1× 10^{-3} M MB with the pH pre-adjusted to 6.0 was added to 29.7 mL BPEI-(SDS/PENS) coacervate. In all cases, the final dye concentration was 0.01 × 10^{-3} M. After stirring for 24 h, samples were centrifuged for 3 h at 8000 rpm (Allegra X-30R Centrifuge, Beckman Coulter). After centrifugation, the supernatant was removed using a micropipette, and the coacervate phase was left in the bottom of centrifuge tubes. The pH of the supernatant was adjusted to pH 6.0 before the UV-vis measurements. UV-vis measurement (Agilent 8453 spectrophotometer) was used to determine the dye concentration in the supernatant and coacervate. The maximum absorbance wavelength for MB, JGB and FL are 664 nm, 608 nm and 475 nm at pH 6.0. The extinction coefficient of MB, JGB and FL at their corresponding maximum absorbance wavelength are 7.24×10^4, 5.23×10^4, and 2.52 ×10^4 $cm^{-1}.M^{-1}$, respectively. The partition coefficient (*K*) was calculated according to equation 1.

$$K = \frac{[Solute\ in\ Coacervate]}{[Solute\ in\ Supernatant]} \qquad (1)$$

2.6 Determination of SDS Micelle Aggregation Number

Fluorescence measurements of SDS solution were performed at excitation and emission wavelengths of 450 and 630 nm respectively, using a Horiba FluoroMax 4 spectrofluorometer, with the addition of $Ru(bipy)_3^{2+}$ as the luminescent donor and 9-MeA as the luminescence quencher. The concentration of the latter in solution was fixed at 1.05 × 10^{-5} M and the concentration of the former was maintained at 7.2 × 10^{-5} M, while the concentration of SDS was varied. The micelle aggregation number (N_{agg}) was obtained by following the previously reported method of Turro and Yekta (equation 2).[52]

$$\left[\ln\left(\frac{I^0}{I}\right)\right]^{-1} = [Q]N_{agg}^{-1}[S]_0 - (cmc/[Q]N) \qquad (2)$$

where I_0 is the emission intensity of the probe $Ru(bipy)_3^{2+}$ in the SDS solution without the addition of the quencher 9-MeA, while *I* is the emission intensity of the probe in the SDS solution with addition of quencher. $[S]_0$ is the concentration of SDS, CMC is the critical micelle concentration of SDS, and [Q] is the quencher concentration added in the SDS solution. The SDS concentration dependence of $Ru(bipy)_3^{2+}$ luminescence intensity is shown in

Fig. S1, which leads to N_{agg} of approximately 60 for SDS, which is comparable with the previously reported aggregation number of SDS.[52,53]

2.7 Determination of Number of SDS Micelles per BPEI Chain

Copper ions can react with the amine groups of the polyethylenimine, to produce a dark blue cuprammonium complex, which exhibits two absorption peaks at 275 and 630 nm as shown in Fig. S2. UV-vis measurement of a series of BPEI-Cu^{2+} complex solutions with the addition of different amounts of BPEI (0 to 0.7 × 10^{-3} M) and the presence of excess copper ions (1 × 10^{-3} M) was performed on Agilent 8453 spectrophotometer, to produce a UV-vis absorbance calibration curve at 275 nm, as shown in Fig. S3a. The UV-vis measurement of the same series of BPEI-Cu^{2+} complex solutions with the presence of 1 mM SDS was carried out as well, to illustrate that the presence of low concentrations of SDS has little impact on the quantification of BPEI concentration (Fig. S3a). The linear fit of absorbance at 275 nm vs. BPEI concentration indicates that forming cuprammonium complex with copper ion is a facile and accurate method to determine BPEI concentration in the solution. The concentration of residual BPEI in the supernatant of each coacervate sample after centrifugation was determined by UV-vis using copper ions as a UV-visible probe of BPEI concentration.

To determine the concentration of SDS in the supernatant, Sudan II was added to the supernatant as a UV-visible probe of SDS concentration. The solutions were prepared by adding 20 mg Sudan II to 10 mL SDS solutions with a variety of SDS concentration to produce a UV-vis absorbance calibration. The solutions were then sonicated for 30 min and then centrifuged at 6000 rpm for 15 min to remove unsolubilized excess dye particles. Then the transparent supernatant was carefully removed using a micropipette. UV-vis measurements of the clear red supernatant were used to generate the absorbance calibration curve, as shown in Fig. S3b. By using this calibration curve, the concentration of SDS in the supernatant could be determined.

The number of SDS micelle per BPEI chain (N) is defined by equation 3.

$$N = \frac{\{[SDS]_{initial} - [SDS]_{supernatant}\}M_n}{\{[BPEI]_{initial} - BPEI_{supernatant}\}M_r N_{agg}} \qquad (3)$$

where $[SDS]_{initial}$ and $[SDS]_{supernatant}$ are the initial concentration in the system and the concentration of SDS residue in the supernatant, M_n is the number average molecular weight of BPEI, [BPEI]initial and [BPEI]supernatant are the initial concentration of BPEI in the system and concentration of BPEI in the supernatant, M_r is the molecular weight of the BPEI repeat unit, and N_{agg} is the aggregation number of SDS micelle, as calculated from section 2.6, which is assumed to be constant throughout the study. Though it has been reported that in some cases polyelectrolyte-surfactant binding can affect the surfactant aggregation number,[54] it has also been reported that when surfactant are in a complex with a weak polyelectrolyte, the impact of the binding on the surfactant aggregation number is much more limited compared to when binding with strong polyelectrolyte.[55] The assumption is therefore made in this study that the aggregation number of SDS micelle remains unchanged at approximately 60, as BPEI is a weak polyelectrolyte.

2.8 ^{1}H NMR

^{1}H NMR of SDS, PENS, and various molar ratios of SDS to PENS using D_2O as the solvent, was carried out on a Mercury 300 spectrometer at a proton resonance frequency of 300 MHz at 30 °C to provide information on the formation of mixed SDS/PENS micelles based on the upfield or downfield shifts of the proton chemical shift of SDS and PENS.

2.9 Simulation of the lipophilic partition coefficient contributions

The pH dependence of the theoretical lipophilic partition coefficient (log*D*) values of the dyes into the coacervates were estimated using the physico-chemical property predictor plugin in MarvinSketch (ChemAxon). This approach followed a previously reported method that used the calculated octanol-water partition coefficient to predict antibiotic activity.[56] Briefly, the partition coefficient of dyes was predicted using a redefinition of the selected atom types to include electron delocalization and the addition of contributions from ionic species. The calculations were dependent on estimates of the pK_a of the ionisable groups, thus the values of log*D* are dependent on pH.

2.10 Rheological measurements

The coacervate samples were prepared as previously discussed by mixing 40 × 10^{-3} M BPEI stock solution (pH = 3.0, 6.0 or 9.0) and 40 × 10^{-3} M SDS stock solution (pH = 3.0, 6.0 or 9.0) with the same pH at various mixing ratio (the details on mixing ratio are shown in Table S1, Supporting Information). In the BPEI-SDS complex coacervate samples, SDS micelles can be regarded as the ionic crosslinkers between the BPEI chains. To present a more straightforward comparison of the impact of pH (or charge density of BPEI) on the rheological property of either the intrapolymer-dominant complex coacervates or the interpolymer-dominant complex coacervates, the factor of SDS micelle number per BPEI chain should be removed by controlling it at a closest value for each intrapolymer-dominant complex coacervate series and interpolymer-dominant coacervate series, respectively (Table S1). The coacervate was collected by centrifuging the mixtures at 8000 rpm for 3 h (Allegra X-30R Centrifuge, Beckman Coulter). The dynamic rheological properties of the coacervates were characterized using a TA Instruments ARES-G2 rheometer in parallel plate geometry using an 8.00 mm diameter aluminium upper plate and 43.9 mm diameter aluminium lower plate along with a solvent trap. For dynamic rheological experiments, a constant strain amplitude of 0.6%, which is within the linear viscoelastic response region for all the collected coacervate samples, was used. The frequency was swept from 0.1 – 100 rad/s for these dynamic measurements.

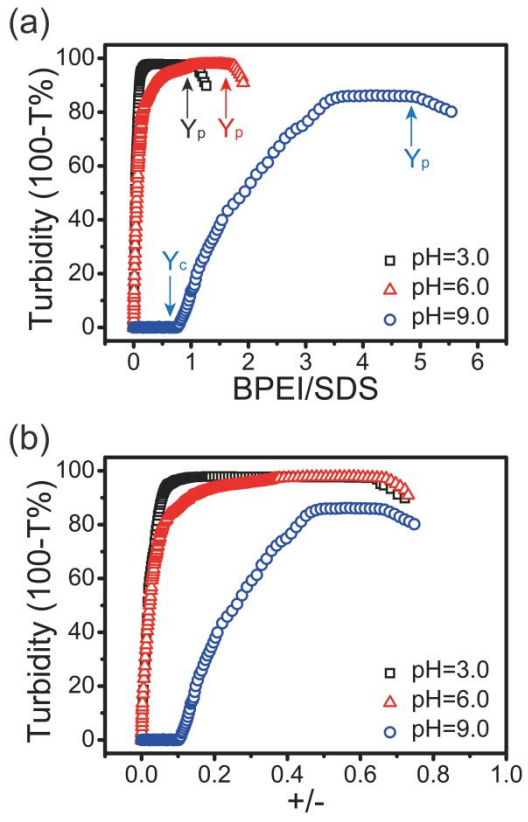

Fig. 2 Turbidity vs. (a) BPEI/SDS ratio and (b) initial +/- charge ratio profiles for BPEI-SDS system, obtained by titrating BPEI (40 × 10^{-3} M) into SDS (40 × 10^{-3} M) stock solutions with the same pH pre-adjusted to 3.0, 6.0 or 9.0. Y_c and Y_p represent the onset of complex coacervation and precipitation in the system, respectively.

3. Results and discussion

3.1 Role of pH on complexation of BPEI and SDS micelles

Turbidity was used to qualitatively assess the complex coacervate formation as a function of pH and the stoichiometry of BPEI to SDS, as shown in Fig. 2a. The charge density of BPEI can be modulated by adjusting solution pH.

The point of initial increase in turbidity is designated as Y_c which represents the onset of complex coacervation in the system, while the point of abrupt decrease in turbidity is indicated as Y_p, which is related to the formation of complexes that precipitate from solution. From the turbidity profile, one can see that the complex coacervation as well as the formation of precipitates is highly dependent on the pH, which means the ionization degree of BPEI. Specifically, a lower pH is associated with higher BPEI ionization degree and leads to an earlier onset of complex coacervation and precipitation with respect to the BPEI/SDS molar ratio, indicating that higher ionization of BPEI promotes both coacervation and precipitation during the titration. The ionization degree of BPEI as a function of pH was determined using potentiometric titration, as shown in Fig. S4. It was assumed that the different types of amine groups have the same ionization constant and did not influence the ionization of the nearby groups. [57,58] Converting the BPEI/SDS stoichiometry to the ratio of positive to negative (+/-) charges as shown in Fig. 2b allows a more direct assessment of the impact of charge compensation. From Fig. 2b, it is obvious that precipitation is strongly dependent on the initial charge ratio rather than BPEI/SDS molar ratio, since the precipitates always form at similar charge ratios (~0.65). The value of this ratio is interesting as precipitation is generally expected to take place at a 1:1 charge ratio.[59] The non-stoichiometry of the insoluble polyelectrolyte complexes is known to occur when weak polyelectrolyte is involved in the complexation.[60] Studies on weak polyelectrolyte multilayer films suggest that (1) at a given pH, the charge density of an adsorbing weak polyelectrolyte can increase substantially from its solution-state value when it is incorporated into a multilayer film and (2) the effective pKa of a weak polyelectrolyte in a multilayer film shifts dramatically from its solution-state value.[61] It is possible that in this BPEI/SDS system there might be pKa shifts of BPEI and enhanced ionization degree of BPEI due to charge-charge interactions, making BPEI more basic.[62] In addition, it was previously shown that the precipitation of oppositely charged polyelectrolytes is concentration dependent, in which a higher total polyelectrolyte concentration promotes precipitation.[33] Therefore, it might be possible that decreasing the total concentration of BPEI and SDS can lead to an increase in Y_p to a value much closer to 1. Unlike in the case for precipitation, charge ratio is not the only dominant factor for coacervation. At pH 3.0 and 6.0, coacervation takes place immediately as the BPEI solution was titrated into SDS solution. However, at pH 9.0, at low BPEI/SDS stoichiometry or charge ratio, there is no

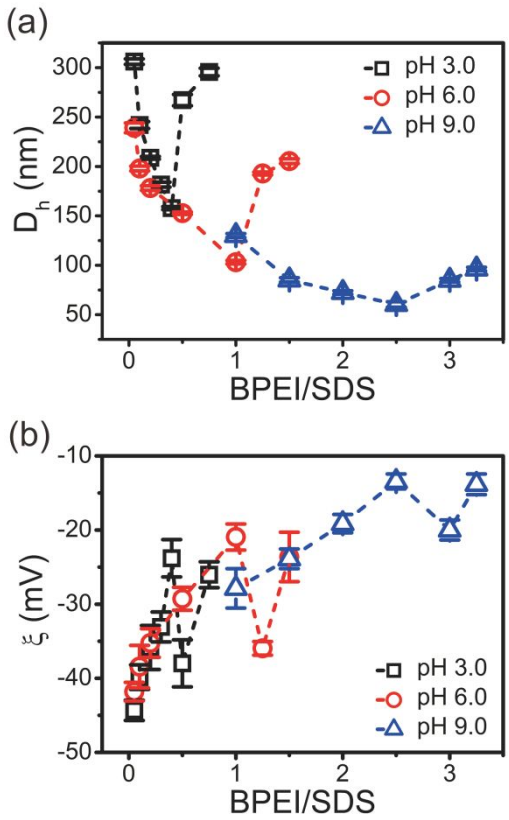

Fig. 3 Hydrodynamic diameter (D_h) and zeta potential (ξ) of BPEI/SDS coacervates as a function of BPEI/SDS stoichiometry and pH. The coacervates were prepared mixing BPEI (40×10^{-3} M) with SDS (40×10^{-3} M) stock solutions with the same pH pre-adjusted to 3.0, 6.0 or 9.0, at different stoichiometry.

coacervate formed. BPEI chains are not highly charged at pH 9.0, with a large spacing between charges along the BPEI chains. There might be some charge "mismatch" between the slightly charged BPEI and SDS at pH 9.0, leading to the shift of Y_c to a higher charge ratio.

3.2 Intrapolymer-dominant vs interpolymer-dominant association

The hydrodynamic diameter and zeta potential of the BPEI-SDS complex coacervates formed at various mixing molar ratios and pH values are shown in Fig. 3. Both the hydrodynamic diameter and zeta potential of the BPEI-SDS coacervates are strongly dependent on the pH. BPEI-SDS coacervates formed at lower pH tend to have a larger particle size and higher absolute value of zeta potential, due to the higher degree of ionization of BPEI at lower pH, allowing it to associate with more SDS micelles. For example, at the same BPEI to SDS stoichiometry of 0.05, the hydrodynamic diameter of the coacervate formed at pH 3.0 is ~300 nm, while that formed at pH 6.0 is ~240 nm. For each series of BPEI/SDS complex coacervates formed at a given pH value, the hydrodynamic diameter of the particles first decreases as the BPEI/SDS molar ratio increases, then at a certain stoichiometry (BPEI/SDS ratio), which are 0.4, 1.0 and 2.5 for pH of 3.0, 6.0 and 9.0, respectively, the size of the coacervates begins to increase, as shown in Fig. 3a. The hydrodynamic size of BPEI-SDS coacervates was also examined as a function of the ratio of positive to negative (+/-) charges, as shown in Fig. S5, in which the charge ratio for the minimum size of BPEI-SDS coacervates is dependent on pH as well. As the pH increases, both the BPEI/SDS molar ratio and the charge ratio (+/-) for the minimum size shift to a larger value. In addition, the zeta potential of BPEI-SDS coacervates initially become less negative as the BPEI/SDS ratio increases until the stoichiometry for the minimum hydrodynamic size of the coacervates is reached. As the BPEI/SDS ratio increases further, an abrupt change in the trend of zeta potential versus BPEI/SDS molar ratio occurs.

To better understand and explain the changes in both hydrodynamic diameter and zeta potential, we propose a model of intrapolymer-dominant and interpolymer-dominant association, as depicted in Fig. 4, which is consistent with previous reports.[1,63,64] In this work, the intrapolymer association and interpolymer association refer to the probability of the association occurring for a given SDS micelle. In the case of intrapolymer association, the SDS micelles associate with a single BPEI chain, while in the case of interpolymer association, the SDS micelles can associate with multiple BPEI chains. The probability of the association mode for BPEI and SDS is dependent on the BPEI/SDS molar ratio. At low BPEI/SDS molar ratio, there are many more SDS micelles than there are BPEI chains, which leads to the formation of BPEI-SDS complexes where the intrapolymer association dominates (intrapolymer-dominant complexation) with a relatively large number of SDS micelles per BPEI chain. With the increase in BPEI-SDS molar ratio, the number of SDS micelles that can be assigned to each BPEI chain decreases, resulting in a decrease in the hydrodynamic diameter as well as the absolute value of the formed coacervates. The decreasing number of SDS micelles per BPEI chain (*N*) for the intrapolymer-dominant complexes with increasing BPEI/SDS mixing ratio also supports this assumption, as shown in Fig. S6, consistent with published studies.[1,63] The number of micelles per BPEI chain in the coacervate phase was decreased from approximately 49 to 11, 32 to 9, and 9 to 6 as the BPEI to SDS stoichiometry increases from 0.05 to 0.4, 0.05 to 1.0 and 1.0 to 2.5 for pH 3.0, 6.0 and 9.0, respectively. For the intrapolymer-dominant complex coacervates, the hydrodynamic diameter of the coacervates decreases as the number of micelles per BPEI chain decreases as shown in Fig. S7. Interestingly, the hydrodynamic diameter collapses as a function of *N* (for intrapolymer-dominant coacervate case) for all pH examined, indicating that the number of micelles per BPEI chain is the dominant factor for the size of coacervates. However, when the BPEI/SDS molar ratio was further increased, for example, at BPEI/SDS stoichiometry of 0.5 for the BPEI-SDS complexes formed at pH 3.0, the association between BPEI and SDS tends to become interpolymer-dominant because of the reduced number of SDS available for each BPEI chain. The number of micelles per BPEI chain for the transform from intrapolymer-dominant complex to interpolymer-dominant complex is pH-dependent, which is approximately 11, 9, and 6 for pH at 3.0, 6.0, and 9.0, respectively.

The electrophoretic mobility of the intrapolymer-dominant BPEI-SDS coacervates was plotted as a function of *N*, as shown in Fig. 5. Irrespective of pH, the absolute values of mobility increase with *N*, since SDS micelles contribute to the negative mobility of the coacervates. Although the trend of mobility vs. *N* is similar for the BPEI-SDS coacervates at different pH, the mobility does not collapse exactly with *N* due to the pH dependent BPEI ionization.

3.3 Partition coefficient of dyes into intrapolymer-dominant BPEI/SDS coacervates

The nonpolar core of micelles allows an enhancement of solubility of hydrophobic materials. In this study, we examined how the type of association between BPEI and SDS as well as the hydrophobicity of the solute itself can influence the uptake ability of these solutes. Three different dyes, MB, FL and JGB, were utilized as representative solutes with different hydrophobicity to determine the solute uptake property of the BPEI-SDS coacervates, using UV-vis measurements. Fig. S8 and Table S2 show the predicted lipophilic partition coefficient values of MB, FL, and JGB as a function of pH, which can be used to evaluate the hydrophobicity of the solutes.[20] The micelle-water partition coefficient of hydrophobic organics has been reported to have a strong positive correlation with the lipophilic partition coefficient.[65] The partition coefficient of MB, FL, and JGB into intrapolymer-dominant BPEI-SDS coacervates at pH 3.0, 6.0, and 9.0 was plotted as a function of the number of SDS micelles per BPEI chain (*N*), as shown in Fig. 6. As shown in Fig. S6, for the dye MB and JGB, the log *D* values are always greater than 0 in the studied pH range from 3.0 to 9.0, which means that these two dyes favour hydrophobic or non-polar environments, while for the dye FL, its log *D* value is highly dependent on the pH. Particularly, at low pH of 3.0, FL favours hydrophobic environment more than the hydrophilic one, while at pH 9.0 it prefers polar environment instead, since the log *D* value is less than 0 at pH 9.0. As shown in Fig. 6, the partition coefficient of dyes into BPEI-SDS coacervates is highly dependent on the hydrophobicity of the dye itself. Specifically, the higher the log

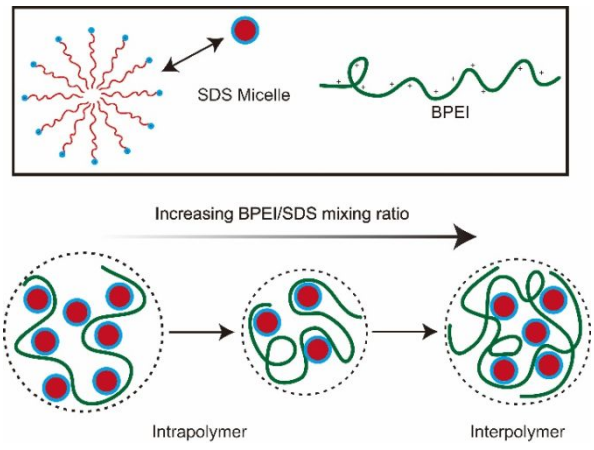

Fig. 4 Schematic illustration of conversion of intrapolymer mode to interpolymer mode as the BPEI/SDS mixing ratio increases.

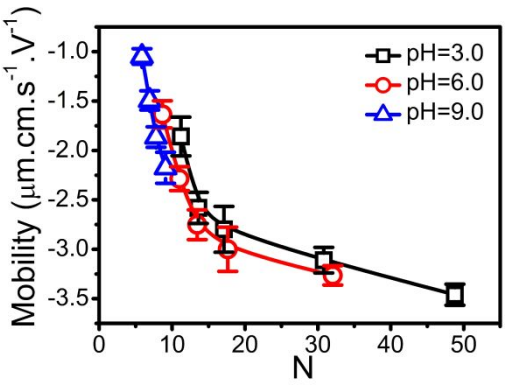

Fig. 5 Electrophoretic mobility of intrapolymer-dominant BPEI-SDS coacervates formed at pH 3.0, 6.0, and 9.0 as a function of number of micelles per BPEI chain (*N*).

D value or the hydrophobicity of the dye, the higher the partition coefficient into BPEI-SDS coacervates is. In addition, for the dyes with a log *D* value larger than 0, their partition coefficient into BPEI-SDS coacervates increases linearly with *N*, indicating that the hydrophobic interaction between SDS and the dye plays an important role in the partitioning process. However, for the dye FL at pH 6.0 and 9.0, the partition coefficient is quite low and decreases with *N*, suggesting that the hydrophobic interaction is not the dominant factor for the solute uptake of the solutes with such a low log *D*. To better explain the decreasing partition coefficient of FL into BPEI-SDS coacervates with *N* at high pH values, the fraction of different charge species of FL was obtained as shown in Fig. S9. At the pH higher than 6.0, the charge of FL molecules is negative, which might be attracted by positively charged BPEI but ejected by negatively charged SDS molecules via electrostatic interaction, as reported in previous studies on the uptake of solutes into polyelectrolyte complexes.[66] Therefore, the competition of sites on the BPEI between SDS and FL as well as the electrostatic repulsion between SDS and FL lead to a lowered partition coefficient as the number of SDS micelles per BPEI chain increases. The lipophilic partition coefficient or hydrophobicity of MB almost does not vary with pH in the pH range from 3.0 to 9.0. Interestingly, the partition coefficient of MB into BPEI-SDS coacervates vs. *N* falls onto the same linear plot, as shown in Fig. 6e, which strongly supports the assumption that the hydrophobicity of the solute is crucial for the partitioning process.

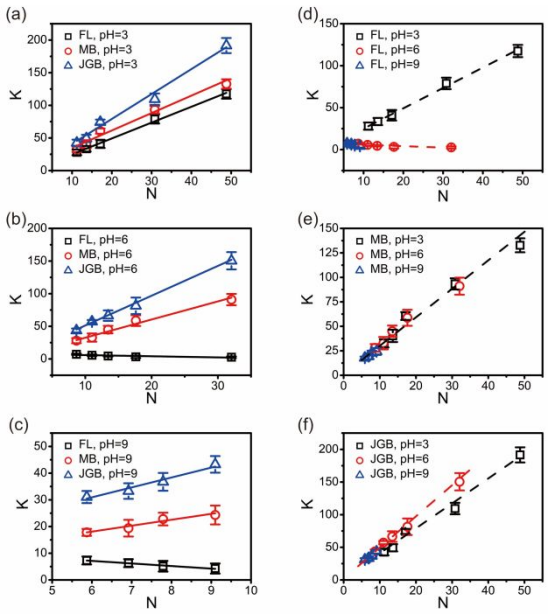

Fig. 6 Partition coefficient K of FL, MB and JGB into intrapolymer-dominant BPEI-SDS coacervates formed at pH (a) 3.0, (b) 6.0, and (c) 9.0 as well as the partition coefficient K of (d) FL, (e) MB and (f) JGB into the coacervates at different pH, as a function of the number of micelles per BPEI chain (*N*),

3.4 Mixed micelles of SDS and PENS

Mixed micelles of SDS and PENS (SDS/PENS) were obtained by mixing SDS and PENS at different molar ratio (SDS:PENS = 1:0, 3.26:1,1.25:1 and 0:1) in D_2O for ^1H NMR measurements, while fixing the total surfactant concentration at 40×10^{-3} M. ^1H NMR has been previously utilized to indicate the formation of mixed micelles. Wang et al. reported that after forming mixed micelles with Trixon-100, the protons of SDS undergoes upfield shift, which is evidence of the ring-current effect of the aromatic phenoxy group of Trixon-100 on the protons of SDS.[67] In this study, similarly, ^1H NMR was applied as well to determine the formation of mixed micelles between SDS and PENS. The ^1H NMR spectra of SDS, PENS and several mixtures of SDS and PENS with different mixing ratio in D_2O were obtained, as shown in Fig. S10. The details on the chemical shifts of SDS and PENS are listed in Table S3. Similarly, because of the ring-current effect of the aromatic phenoxy group of PENS, the chemical shift of SDS protons also undergoes a upfield shift as the fraction of PENS in the system increases, which suggests the mixed micellization of SDS and PENS.

The hydrodynamic diameter of mixed micelles was investigated using DLS measurement at various mixing ratios, as shown in Fig. S11. As the molar fraction of PENS increases, the hydrodynamic diameter of the micelles increases gradually from approximately 3.0 to 4.5 nm.

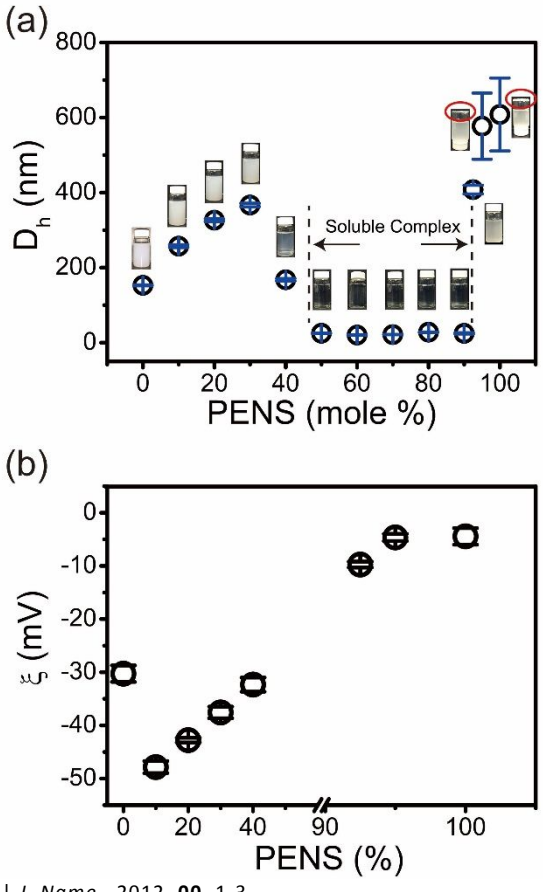

Fig. 7 Hydrodynamic diameter (D_h) and zeta potential (ξ) of BPEI-SDS coacervates as a function of PENS mole fraction of total surfactant. The coacervates were prepared by mixing BPEI (40×10^{-3} M) solutions with SDS/PENS mixtures (40×10^{-3} M) with the same pH pre-adjusted to 6.0, at a fixing BPEI to surfactant stoichiometry of 0.5.

3.5 Complexation of BPEI with the mixed micelles

Complexation of BPEI with mixed SDS/PENS micelles prepared at different PENS content with a fixed total surfactant concentration of 40×10^{-3} M, was studied at pH 6.0, at a fixed ratio of BPEI/(SDS/PENS) of 0.5 in the initial solutions. The hydrodynamic diameter as well as the zeta potential of the BPEI-(SDS/PENS) complexes was measured, as shown in Fig. 7. PENS% is defined as shown in equation 4 to better illustrate the composition of the mixed micelles.

$$\text{PENS\%} = n_{PENS}/(n_{SDS} + n_{PENS}) \times 100\% \quad (4)$$

where n_{PENS} and n_{SDS} represents the number of moles of SDS and PENS in the mixed micelle system.

As shown in Fig. 7a, at low PENS mole fraction (0 – 40%), BPEI undergoes complex coacervation with SDS/PENS mixed micelles, with hydrodynamic diameter increasing from ~150 nm to 365 nm as the PENS mole fraction increases from 0 to 40%. Upon consideration of the zeta potential values of the solution after complex coacervate has occurred (with that phase dispersed in the water rich phase) at low PENS mole fraction (0 – 40%), one sees a maximum in the absolute value of zeta potential at ~-48 mV for the BPEI-(SDS/PENS) complex coacervate formed at PENS% = 10%. We further propose that at this condition, with the addition of PENS into the system, the mixed micelles tend to form interpolymer-dominant complexes with BPEI rather than the intrapolymer-dominant complexes formed in the pure SDS micelle case. The increase in hydrodynamic diameter with PENS mole fraction is probably due to the formation of interpolymer-dominant complexes between BPEI and SDS/PENS mixed micelles at 40% ≥ PENS% ≥ 10%. In addition, the maximum absolute value of zeta potential at PENS% = 10% occurs because of the conversion from the intrapolymer-dominant complexes of the BPEI-SDS system to interpolymer-dominant complexes for BPEI-(SDS/PENS) system.

However, when the PENS% is between 50% – 90%, complex coacervation process does not occur, as can be seen from the inset pictures in Fig. 7a. In order to better understand the

association or interaction between BPEI and the SDS/PENS mixed micelles formed when the PENS mole fraction is from 50% – 90%, detailed information on the size distribution of particles in these systems as well as BPEI at pH 6.0 was obtained, shown in Fig. S12. The particle size measured for BPEI in dilute aqueous solution at pH 6.0 is always smaller than the particles in BPEI-(SDS/PENS) solution, indicating that there is some loose association between the SDS/PENS mixed micelles and BPEI chain although complex coacervation does not occur. A possible explanation for suppression of phase separation at intermediate PENS% is proposed in this study. It could be possible that the packing of surfactant head groups is less efficient for SDS/PENS mixed micelles than the SDS micelles, resulting in lower extent of micellar counterion condensation in the mixed micelles. The entropic driving force for mixed micelle-BPEI complexation is therefore diminished, leading to the suppression of phase separation at intermediate PENS%.

When the PENS% is greater than 92.5%, phase separation occurs again. A coacervate formed at the PENS% of 92.5%, while precipitates formed at the PENS% of 95% and 100%. It is generally not considered that a second phase transition, liquid to solid, is occurring when precipitation is seen,[41,68,69] but rather these cases indicate strong association between the oppositely charged moieties (e.g. strong oppositely charged polyelectrolytes)[41,69] or that an increased hydrophobicity of the precipitating system.[70,71] The point at which precipitates form can also be seen as the point at which the colloidally stable dispersion of complex coacervate droplets is destabilized. As shown in Fig. S13, the hydrodynamic diameter of the SDS-PENS complexes formed using BPEI and mixed micelles with a PENS% of 95% and 100% increases dramatically within several minutes, suggesting that this phase separation might be kinetically controlled.[41] The low value of the zeta potential of BPEI-PENS complexes accelerates the aggregation and precipitation process. Another study on the complexation of PEI-SDS also reveals that the precipitation of PEI-SDS complexes is a result of both the increased hydrophobicity of the complexes and the low zeta potential of the complexes which leads to the coagulation of the PEI-SDS system.[46]

To better understand how the mixed micelle composition influences the phase behaviour of the BPEI-mixed surfactant system, turbidimetric titration of BPEI into surfactant as a function of increasing BPEI/surfactant ratio is shown in Fig. S14. First of all, the BPEI-surfactant coacervate regime narrows with an increase in PENS%, indicating that the dispersion of BPEI-surfactant coacervate droplets is destabilized when the PENS% is increased. The destabilization of BPEI-surfactant coacervates as PENS% increases is probably due to the increased hydrophobicity produced by PENS. An interesting phenomenon is the titration of BPEI into 30% PENS surfactant solution, which undergoes a coacervation-partial dissolution-precipitation process. The coacervates formed immediately as the BPEI was titrated into surfactant solution, and as the BPEI/surfactant ratio reaches approximately 1.6, the turbidity of the system was reduced significantly with no precipitation, which indicates that the coacervate partially dissolves. However, when the BPEI/surfactant ratio was increased to ~2.0, the cloudiness of the BPEI-surfactant system increases significantly and precipitates were formed instead. Another interesting finding is that the coacervate does not form for BPEI-70% PENS surfactant system until the stoichiometry of BPEI to surfactant reaches approximately 1.5.

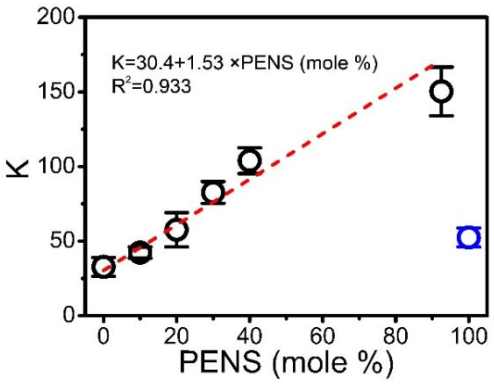

Fig. 8 Partition coefficient (*K*) of MB into BPEI-(SDS/PENS) coacervates as a function of PENS mole fraction of total surfactant. The coacervates were prepared by mixing BPEI (40×10^{-3} M) solutions with SDS/PENS mixtures (40×10^{-3} M) with the same pH pre-adjusted to 6.0, at a fixing BPEI to surfactant stoichiometry of 0.5. Then 0.01×10^{-3} M MB was added to this system.

3.5 Role of PENS on the uptake of MB

It has been reported that the length and architecture of the hydrophobic tails of surfactants has an impact on the uptake of dyes. Micelles formed using surfactants with a longer and linear tail show more efficient uptake of hydrophobic dyes than the micelles formed using surfactant with shorter and branched tail.[35,36,50,51] The chain length of PENS is much larger than that of SDS, chemical structures shown in Fig. S14, which means that the micelles formed with more PENS should have a higher MB uptake ability. Additionally, the aromatic functional group of PENS may also enable π-π interaction between PENS and MB, contributing to the higher uptake of MB into the complex coacervate phase as well. To study the influence of PENS on the uptake of MB, the partition coefficient into BPEI-(SDS/PENS) coacervates was plotted as a function of PENS mole fraction of the total surfactant, as shown in Fig. 8. The partition coefficient of MB into the BPEI-(SDS/PENS) complex coacervate phase increases almost linearly except where precipitates are formed. For the 100% PENS case, the dye taken into the precipitate is less than the amount of dye taken into the complex coacervate phase for 92.5% PENS mixed micelles, showing that partitioning into a complex coacervate phase can be more effective than directly flocculating the small molecule from solution. The network for precipitates is usually tighter than that for coacervates.[72] As the tighter, or more crosslinked, network might slow the diffusion of solutes into the precipitate, a question that arises is whether the system is at equilibrium when we measure the partition coefficient in the case of precipitation. To answer this question, the partition coefficient of MB into the precipitate was measured after 3 days as well, which remains unchanged over time, indicating that the partition coefficient measured in this study is at equilibrium. The lower partition coefficient of MB in the precipitate is likely

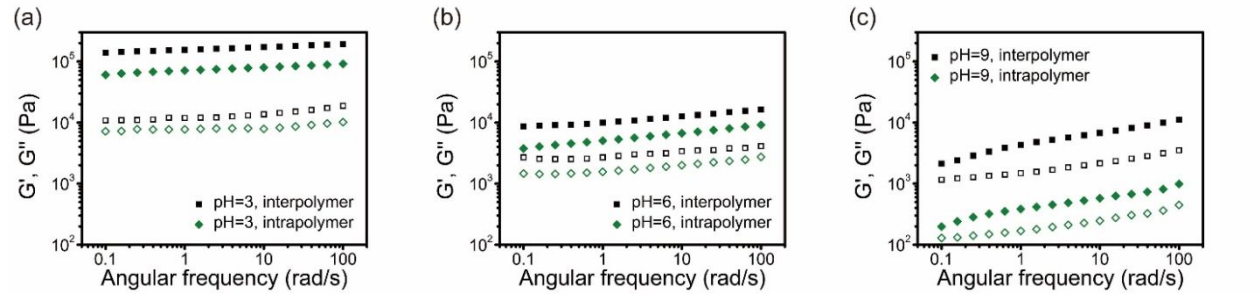

Fig. 9 Frequency sweeps showing storage (G', solid) and loss (G'', open) modulus of BPEI-SDS coacervates formed at different pH and association mode. The intrapolymer-dominant coacervates are prepared by mixing BPEI with SDS micelles with a molar ratio of 0.4, 0.5 and 1.0 for pH at 3.0, 6.0 and 9.0, respectively. The interpolymer-dominant coacervates are prepared by mixing BPEI with SDS micelles with a molar ratio of 1.0, 1.25, and 3.0 for pH at 3.0, 6.0 and 9.0, respectively. The BPEI to SDS molar ratio was selected to have a close number of micelles per BPEI chain for either the intrapolymer-dominant or interpolymer-dominant coacervate series at different pH.

due to the reduced number of available binding sites for MB and steric hindrance effect for MB induced by the tighter network.[73,74] Although this might be a kinetic effect rather than thermodynamic, the kinetics have essentially "frozen" the system, and it seems the measured partition coefficients are meaningful quantifications of the properties of these systems These results indicate that the PENS content in the mixed micelle complex coacervate plays a crucial role in its solute uptake ability.

3.6 Rheological Properties of BPEI-SDS coacervates

A variety of factors including salt concentration, polyelectrolyte stoichiometry, pH, polymer chain length, as well as the chain length matching have been shown to have an influence on the rheological properties of polyelectrolyte complexes as well as polyelectrolyte coacervates.[75–81] In this study, to study how the charge density or pH, and the different association mode (intrapolymer-dominant or interpolymer-dominant complex) influence the rheological behaviour of the BPEI-SDS coacervates, a series of BPEI-SDS coacervates were prepared (see Table S1) and further investigated by using dynamic rheological measurements. The dynamic moduli, G' and G'', are presented as a function of frequency for the complex BPEI-SDS coacervates. The experiments were performed at a constant strain of 0.6%, which was found to be in the linear regime. The viscoelastic behaviour of the formed coacervates are highly dependent on the charge density of BPEI as well if the association of BPEI-SDS complex is intrapolymer-dominant or interpolymer-dominant, as shown in Fig. 9. Remarkably, for all the BPEI-SDS complex coacervates formed at pH 3.0, 6.0, and 9.0, the storage modulus (G') is significantly higher than the loss modulus (G'') at all the frequencies measured, (e.g., $\tan\delta << 1$), as shown in Fig. 10, indicating that the as-prepared BPEI-SDS coacervates form an interconnected gel-like network. In this study, SDS micelles are regarded as the ionic crosslinker between BPEI chains.

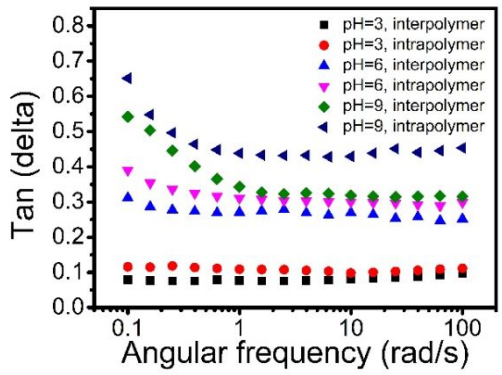

Fig. 10 Loss tangent ($\tan\delta = G''/G'$) of the intrapolymer-dominant and interpolymer-dominant coacervates at different pH. The intrapolymer-dominant coacervates are prepared by mixing BPEI with SDS micelles with a molar ratio of 0.4, 0.5 and 1.0 for pH at 3.0, 6.0 and 9.0, respectively. The interpolymer-dominant coacervates are prepared by mixing BPEI with SDS micelles with a molar ratio of 1.0, 1.25, and 3.0 for pH at 3.0, 6.0 and 9.0, respectively.

BPEI charge density or pH has been shown to have a strong influence on the rheological properties of polyelectrolyte complexes.[82] Specifically, as the pH decreases, the modulus of BPEI-SDS coacervates increases dramatically, which is probably due to a higher interconnection between the more charged BPEI and SDS. The increased modulus of PBEI-SDS coacervates at lower pH indicates that there tends to be more ionic bonds between BPEI and SDS for the coacervates formed at lower pH. For the BPEI-SDS coacervates formed at the same pH value but with different association mode (intrapolymer-dominant or interpolymer-dominant complex), the viscoelastic behaviour is quite different. At each pH value, the formed interpolymer-dominant complex coacervates show higher storage moduli as well as lower $\tan\delta$ values than the intrapolymer-dominant complex coacervates. These characteristics are consistent with the formation of more ionic crosslinks between different polymer chains in the polyelectrolyte complex.[77] It may be initially unclear why interpolymer-dominant complex coacervates would form more ionic crosslinks than the intrapolymer-dominant coacervates, since the number of SDS micelles per BPEI chain is lower in the interpolymer-dominant coacervates. However, the interpolymer associations can be considered as effective crosslinks, while the intrapolymer associations effectively generate loops from a polymer network perspective. In the intrapolymer-dominant coacervates, the

SDS micelle tends to dominantly form ionic bonds with one BPEI chain and these bonds would not contribute to the formation of an ionic network to support stresses. These intrapolymer bonds should be equivalent to the formation of loops in a network polymer. This concept is supported by the higher tan δ value, i.e., more energy dissipations.[83] In the interpolymer-dominant coacervates, the SDS micelle tends to dominantly form ionic bonds with multiple BPEI chains, leading to the formation of effective crosslinks in the network. Therefore, in the context of effective ionic crosslinks, it is not surprising that the interpolymer-dominant coacervates have a higher storage modulus and lower $\tan\delta$ than the intrapolymer-dominant complexes despite the lower number of micelles per BPEI chain for the interpolymer-dominant complex coacervates.

Conclusions

Presented here is a study of the phase behaviour and formation of intrapolymer-dominant and interpolymer-dominant polyelectrolyte-micelle and polyelectrolyte-mixed micelle coacervates, their ability to uptake dye, and the rheological properties of these coacervates. BPEI-SDS complex coacervates were formed by simply mixing BPEI and SDS stock solutions with the same pH at different mixing ratios. The influence of pH, or charge density of BPEI, as well as mixing molar ratio was measured with turbidity, DLS, and zeta potential. It was seen that charge ratio is key in precipitation of this system. Based on the variation of coacervate size and zeta potential with BPEI/SDS mixing ratio, an intra- vs interpolymer association model was proposed. Specifically, intrapolymer-dominant complex coacervates were formed at low BPEI/SDS molar ratio, while at high BPEI/SDS molar ratio BPEI and SDS tend to form interpolymer-dominant complex coacervates instead. The number of SDS micelles per BPEI chain can be assigned. Complexation of BPEI with the mixed SDS/PENS micelles shows different phase behaviour than the BPEI-SDS. Based on the zeta potential and hydrodynamic diameter data, it can be inferred that at 40% ≥PENS % ≥10% with a BPEI to mixed micelle ratio of 0.5, the mixed micelles tend to form interpolymer-dominant complexes with BPEI rather than intrapolymer-dominant complexes for the pure SDS micelles. However, when the proportion of PENS in the mixed micelle is 50% – 90%, BPEI tends to form a loose association with the mixed micelles, rather than undergoing the coacervation. For the complexes formed using BPEI and mixed micelles with a composition of 95% or 100 % PENS, the association is strong and form precipitates.

Partition coefficient of four different dyes into BPEI-SDS intrapolymer-dominant coacervates was studied as a function of pH and mixing ratio. An increase in dye hydrophobicity and the number of SDS micelles per BPEI chain leads to a higher partition coefficient. In addition, by using mixed SDS/PENS micelles instead of SDS micelles, the partition coefficient of MB into coacervates can be enhanced probably because of the more hydrophobic environment produced by the surfactant PENS.

Dynamic rheological measurements on the coacervates suggest that the rheological properties of the complex coacervates are impacted by the association mode of the coacervates as well as the charge density of BPEI chains. An increase in the charge density of BPEI chains results in a higher ionic bond density between BPEI and SDS micelles, therefore more solid-like behaviour. Even for the BPEI-SDS coacervates formed at the same pH value, the interpolymer-dominant coacervates shows a much higher modulus and lower $\tan\delta$ value, indicating that there are more effective ionic network bonds in the interpolymer-dominated complexes than the intrapolymer-dominant complexes.

Conflicts of interest

There are no conflicts to declare.

Acknowledgements

The authors would like to acknowledge support from NSF award DMR-1425187 and CMMI-1462284. The authors would also like to thank Prof. Xiong Gong of the University of Akron for use of his UV-vis equipment.

Reference

1 J. Xia, H. Zhang, D. R. Rigsbee, P. L. Dubin and T. Shaikh, *Macromolecules*, 1993, **26**, 2759–2766.
2 E. Kizilay, A. B. Kayitmazer and P. L. Dubin, *Adv. Colloid Interface Sci.*, 2011, **167**, 24–37.
3 Y. Lapitsky, T. Zahir and M. S. Shoichet, *Biomacromolecules*, 2008, **9**, 166–174.
4 Y. Lapitsky, W. J. Eskuchen and E. W. Kaler, *Langmuir*, 2006, **22**, 6375–6379.
5 M. J. Voorn, *Recueil*, 1956, **75**, 317–330.
6 H. Wang, Y. Wang, H. Yan, J. Zhang and R. K. Thomas, *Langmuir*, 2006, **22**, 1526–1533.
7 Y. Wang, K. Kimura, P. L. Dubin and W. Jaeger, *Macromolecules*, 2000, **33**, 3324–3331.
8 Y. Wang, K. Kimura, Q. Huang, P. L. Dubin and W. Jaeger, *Macromolecules*, 1999, **32**, 7128–7134.
9 B. S. Kim, S. W. Park and P. T. Hammond, *ACS Nano*, 2008, **2**, 386–392.
10 J. Jiang, G. Wang, Y. Ma, Z. Cui and B. P. Binks, *Soft Matter*, 2017, **13**, 2727–2732.
11 S. Son, E. Shin and B. S. Kim, *Biomacromolecules*, 2014, **15**, 628–634.
12 H. Oh, A. M. Ketner, R. Heymann, E. Kesselman, D. Danino, D. E. Falvey and S. R. Raghavan, *Soft Matter*, 2013, **9**, 5025.
13 T. S. Davies, A. M. Ketner and S. R. Raghavan, *J. Am. Chem. Soc.*, 2006, **128**, 6669–6675.
14 Y. Zhang, Y. Han, Z. Chu, S. He, J. Zhang and Y. Feng, *J. Colloid Interface Sci.*, 2013, **394**, 319–328.
15 A. Mezei, R. Mészáros, I. Varga and T. Gilányi, *Langmuir*, 2007, **23**, 4237–4247.
16 L. Chiappisi, S. David Leach and M. Gradzielski, *Soft Matter*, 2017, **13**, 4988–4996.
17 M. Zhao, S. A. Eghtesadi, M. B. Dawadi, C. Wang, S. Huang, A. E. Seymore, B. D. Vogt, D. A. Modarelli, T. Liu and N. S. Zacharia, *Macromolecules*, 2017, **50**, 3818–3830.

18 K. A. Black, D. Priftis, S. L. Perry, J. Yip, W. Y. Byun and M. Tirrell, *ACS Macro Lett.*, 2014, **3**, 1088–1091.
19 M. Zhao and N. S. Zacharia, *Macromol. Rapid Commun.*, 2016, **37**, 1249–1255.
20 K. Lv, A. W. Perriman and S. Mann, *Chem. Commun.*, 2015, **51**, 8600–8602.
21 L. Yu, X. Liu, W. Yuan, L. J. Brown and D. Wang, *Langmuir*, 2015, **31**, 6351–6366.
22 Y. Xu, M. Mazzawi, K. Chen, L. Sun and P. L. Dubin, *Biomacromolecules*, 2011, **12**, 1512–1522.
23 T.-Y. Dora Tang, C. Rohaida Che Hak, A. J. Thompson, M. K. Kuimova, D. S. Williams, A. W. Perriman and S. Mann, *Nat. Chem.*, 2014, **6**, 527–533.
24 P. Stano and P. L. Luisi, *Chem. Commun.*, 2010, **46**, 3639–3653.
25 K. Kurihara, M. Tamura, K. Shohda, T. Toyota, K. Suzuki and T. Sugawara, *Nat. Chem.*, 2011, **3**, 775–781.
26 S. S. Mansy, J. P. Schrum, M. Krishnamurthy, S. Tobé, D. A. Treco and J. W. Szostak, *Nature*, 2008, **454**, 122–125.
27 B. Städler, A. D. Price, R. Chandrawati, L. Hosta-Rigau, A. N. Zelikin and F. Caruso, *Nanoscale*, 2009, **1**, 68–73.
28 C. Wu, S. Bai, M. B. Ansorge-Schumacher and D. Wang, *Adv. Mater.*, 2011, **23**, 5694–5699.
29 A. B. Subramaniam, J. Wan, A. Gopinath and H. A. Stone, *Soft Matter*, 2011, **7**, 2600–2612.
30 P. L. Luisi, F. Ferri and P. Stano, *Nat. Life Class. Contemp. Perspect. from Philos. Sci.*, 2010, 272–288.
31 A. J. Dzieciol and S. Mann, *Chem. Soc. Rev.*, 2012, **41**, 79–85.
32 D. Priftis, R. Farina and M. Tirrell, *Langmuir*, 2012, **28**, 8721–8729.
33 S. Huang, M. Zhao, M. B. Dawadi, Y. Cai, Y. Lapitsky, D. A. Modarelli and N. S. Zacharia, *J. Colloid Interface Sci.*, 2018, **518**, 216–224.
34 Y. Lapitsky and E. W. Kaler, *Soft Matter*, 2006, **2**, 779–784.
35 A. R. Tehrani-Bagha and K. Holmberg, *Materials (Basel).*, 2013, **6**, 580–608.
36 A. R. Tehrani-Bagha, R. G. Singh and K. Holmberg, *Colloids Surfaces A Physicochem. Eng. Asp.*, 2013, **417**, 133–139.
37 K. Thalberg, B. Lindman and G. Karlström, *J. Phys. Chem.*, 1991, **95**, 3370–3376.
38 N. Jain, S. Trabelsi, S. Guillot, D. McLoughlin, D. Langevin, P. Letellier and M. Turmine, *Langmuir*, 2004, **20**, 8496–8503.
39 Y. Li, J. Xia and P. L. Dubin, *Macromolecules*, 1994, **27**, 7049–7055.
40 P. L. Dubin, D. R. Rigsbee, L. M. Gan and M. A. Fallon, *Macromolecules*, 1988, **21**, 2555–2559.
41 F. Comert, D. Nguyen, M. Rushanan, P. Milas, A. Y. Xu and P. L. Dubin, *J. Phys. Chem. B*, 2017, **121**, 4466–4473.
42 P. L. Dubin and R. Oteri, *J. Colloid Interface Sci.*, 1983, **95**, 453–461.
43 J. Xia, H. Zhang, D. R. Rigsbee, P. L. Dubin and T. Shaikh, *Macromolecules*, 1993, **26**, 2759–2766.
44 Y. Wang, K. Kimura, Q. Huang and P. L. Dubin, *Macromolecules*, 1999, **32**, 7128–7134.
45 D. W. McQuigg, J. I. Kaplan and P. L. Dubin, *J. Phys. Chem.*, 1992, **96**, 1973–1978.
46 R. Mészáros, L. Thompson, M. Bos, I. Varga and T. Gilányi, *Langmuir*, 2003, **19**, 609–615.
47 A. Mezei, Á. Ábrahám, K. Pojják and R. Mészáros, *Langmuir*, 2009, **25**, 7304–7312.
48 G. Petzold and S. Schwarz, *Sep. Purif. Technol.*, 2006, **51**, 318–324.
49 S. Chatterjee, M. W. Lee and S. H. Wooa, *Bioresour. Technol.*, 2010, **101**, 1800–1806.
50 M. Abu-Hamdiyyah and I. a. Rahman, *J. Phys. Chem.*, 1985, **89**, 2377–2384.
51 B. Haldar, A. Chakrabarty, A. Mallick, M. C. Mandal, P. Das and N. Chattopadhyay, *Langmuir*, 2006, **22**, 3514–3520.
52 N. J. Turro and A. Yekta, *J. Am. Chem. Soc.*, 1978, **100**, 5951–5952.
53 B. Hammouda, *J. Res. Natl. Inst. Stand. Technol.*, 2013, **118**, 151.
54 P. Hansson and M. Almgren, *J. Phys. Chem.*, 1996, **100**, 9038–9046.
55 K. Thalberg, J. van Stam, C. Lindblad, M. Almgren and B. Lindman, *J. Phys. Chem.*, 1991, **95**, 8975–8982.
56 V. N. Viswanadhan, A. K. Ghose, G. R. Revankar and R. K. Robins, *J. Chem. Inf. Comput. Sci.*, 1989, **29**, 163–172.
57 X. Huang, A. B. Schubert, J. D. Chrisman and N. S. Zacharia, *Langmuir*, 2013, **29**, 12959–12968.
58 J. Suh, H.-J. Paik and B. K. Hwang, *Bioorg. Chem.*, 1994, 22, 318–327.
59 E. Kizilay, a. B. Kayitmazer and P. L. Dubin, *Adv. Colloid Interface Sci.*, 2011, **167**, 24–37.
60 W. Arguelles-Monal, M. Garciga and C. Peniche-Covas, *Polym. Bull.*, 1990, **23**, 307–313.
61 J. Choi and M. F. Rubner, *Macromolecules*, 2005, **38**, 116–124.
62 A. B. Kayitmazer, A. F. Koksal and E. Kilic Iyilik, *Soft Matter*, 2015, **11**, 8605–8612.
63 J. Xia, P. L. Dubin and Y. Kim, *J. Phys. Chem.*, 1992, **96**, 6805–6811.
64 Y. Li, P. L. Dubin, H. A. Have1, S. L. Edwards and H. Dautzenberg, *Langmuir*, 1995, **11**, 2486–2492.
65 K. T. Valsaraj and L. J. Thobodeaux, 1989, **23**, 183–189.
66 P. Tirado, A. Reisch, E. Roger, F. Boulmedais, L. Jierry, P. Lavalle, J. C. Voegel, P. Schaaf, J. B. Schlenoff and B. Frisch, *Adv. Funct. Mater.*, 2013, **23**, 4785–4792.
67 T.-Z. Wang, S.-Z. Mao, X.-J. Miao, S. Zhao, J.-Y. Yu and Y.-R. Du, *J. Colloid Interface Sci.*, 2001, **241**, 465–468.
68 F. Comert and P. L. Dubin, *Adv. Colloid Interface Sci.*, 2017, **239**, 213–217.
69 F. Comert, A. J. Malanowski, F. Azarikia and P. L. Dubin, *Soft Matter*, 2016, **12**, 4154–4161.
70 E. Tsuchida, *J. Macromol. Sci. Part A*, 1994, **31**, 1–15.
71 K. Abe, H. Ohno and E. Tsuchida, *Makromol. Chem.*, 1977, **178**, 2285–2293.
72 R. Chollakup, J. B. Beck, K. Dirnberger, M. Tirrell and C. D. Eisenbach, *Macromolecules*, 2013, **46**, 2376–2390.
73 M. J. Lazzara, D. Blankschtein and W. M. Deen, *J. Colloid Interface Sci.*, 2000, **226**, 112–122.
74 X. L. Wang, T. Tsuru, S. I. Nakao and S. Kimura, *J. Memb. Sci.*, 1997, **135**, 19–32.

75 C. Wang, Y. Duan, N. S. Zacharia and B. D. Vogt, *Soft Matter*, 2017, **13**, 1161–1170.
76 M. W. Liberatore, N. B. Wyatt, M. Henry, P. L. Dubin and E. Foun, *Langmuir*, 2009, **25**, 13376–13383.
77 H. Zhang, C. Wang, G. Zhu and N. S. Zacharia, *ACS Appl. Mater. Interfaces*, 2016, **8**, 26258–26265.
78 E. Spruijt, M. A. Choen Stuart and J. Van Der Gucht, *Macromolecules*, 2013, **46**, 1633–1641.
79 X. Wang, J. Lee, Y. Wang and Q. Huang, *Biomacromolecules*, 2007, **8**, 992–997.
80 D. Priftis, K. Megley, N. Laugel and M. Tirrell, *J. Colloid Interface Sci.*, 2013, **398**, 39–50.
81 Q. Ru, Y. Wang, J. Lee, Y. Ding and Q. Huang, *Carbohydr. Polym.*, 2012, **88**, 838–846.
82 A. Alemdar, N. Öztekin, F. B. Erim, Ö. I. Ece and N. Güngör, *Bull. Mater. Sci.*, 2005, **28**, 287–291.
83 C. Wang, C. G. Wiener, Z. Cheng, B. D. Vogt and R. A. Weiss, *Macromolecules*, 2016, **49**, 9228–9238.